Far-Echo Cancellation in the Presence of Frequency Offset

THOMAS F. QUATIERI, SENIOR MEMBER, IEEE, AND GERALD C. O'LEARY, MEMBER, IEEE

Abstract—**In this paper, we present a design for a full-duplex echo-cancelling data modem based on a combined adaptive reference echo canceller and adaptive channel equalizer. The adaptive reference algorithm has the advantage that interference to the echo canceller caused by the far-end signal can be eliminated by subtracting an estimate of the far-end signal based on receiver decisions. This technique provides a new approach for full-duplex far-echo cancellation in which the far echo can be cancelled in spite of carrier frequency offset. To estimate the frequency offset, the system uses a separate receiver structure for the far echo which provides equalization of the far-echo channel and tracks the frequency offset in the far echo. The feasibility of the echo-cancelling algorithms is demonstrated by computer simulation with realistic channel distortions and with 4800 bits/s data transmission at which rate frequency offset in the far echo becomes important.**

I. Introduction

ADAPTIVE echo cancellers are used in high speed ($\geq$4800 bits/s) full-duplex voice band data transmission to suppress both the near and far echoes which occur on the telephone connection [1]–[4]. These echoes are usually generated by the two-to-four wire hybrid conversions at each end of the telephone channel. Besides dealing with these echoes, a modem operating on a telephone channel must deal with other distortions such as dispersion in the channel, carrier frequency offsets in each direction on the channel, abrupt carrier phase changes (phase hits), and phase jitter [1], [3]–[5]. In addition to such anomalies, the adaptive echo cancellers must contend with interference from the wanted far-end signal ("double-talk"), and interference among the echoes themselves [6].

In this paper, we describe an algorithm which extends the adaptive reference echo canceller (AREC) proposed by Falconer [7], to allow for the cancellation of far echoes with frequency offsets. In the AREC approach to echo cancellation, the interference from each interference source is eliminated by subtracting an estimate derived from the receiver demodulation decisions.

Elimination of the far echo with frequency offset is a difficult problem. The far echo is typically smaller than the desired far-end signal, but not so small that it does not affect the receiver's ability to demodulate the signal. The far echo actually becomes one of the limiting factors in receiver performance at 4800 bits/s and above [1]. The elimination of the far echo is further complicated by the fact that it has traversed the channel twice and has been subjected to the distortions and frequency offset uncertainties of each direction. In particular, carrier frequency offset can be the most damaging to far-echo cancellation; errors as small as 2 Hz, not atypical of a telephone channel, cause serious degradation in performance of echo cancellers.

In this paper, we generalize the AREC technique to eliminate the far-echo interference. The basic technique is to first enhance the visibility of the far echo by subtracting estimates of the two major interfering signals, the near echo and the far signal. A separate adaptive-receiver structure is then used to demodulate the enhanced far-echo signal and make an estimate of its frequency offset. Once this offset is determined, adaptive cancellation of the far echo is possible in the same way that the near echo is cancelled. The feasibility of the complete system is demonstrated by simulation under a wide range of realistic operating conditions which include frequency offset, white Gaussian and impulse noise, and phase hits.

The paper is organized as follows. First, we review the channel model and the various sources of interference and describe the limitations of conventional cancellation techniques. We then describe the operation of the AREC canceller, proposed by Falconer [7] for near-echo cancellation, and show why this structure is not suitable for cancellation when either the far echo or desired far signal are corrupted by frequency offset. The AREC technique is then modified—using a conventional frequency offset tracking receiver—to estimate frequency offset in the far signal. This modification motivates the new AREC configuration which cancels far echo with frequency offset. The results of a simulation which verify the performance of the algorithm are then presented and compared to an approximate analytic model of the steady-state behavior of the system.

II. Formulation

A. Channel Model

Fig. 1 shows the model of the echo channel. The two modems exchange data over a full-duplex telephone channel. Each modem contains a transmitter (modulator) and receiver (demodulator) and is connected to the local central office by a two-wire local subscriber loop. A hybrid coupler is used at each end of the subscriber loop to convert between the two-wire bidirectional loop and the four-wire circuits of the modem and the telephone plant. Reflections generated at these hybrids are the principal source of echos.

Assume that the far-end transmitted signal is a multiphase PSK signal [8]. In a sampled data system, the resulting transmitted signal is given by

$$s_{tf}(nT) = \mathrm{Re} \sum_k I_{tf}^k p((n-kL)T) \exp [j\omega_c nT] \quad (1)$$

where $p(nT)$ is the value of the transmitter shaping pulse at time nT, L is the symbol or baud interval in samples, the value I_{tf}^k which conveys the transmitted information of the kth baud is a complex value selected from the transmitter signal constellation, and $\omega_c/2\pi$ is the carrier frequency. When the transmit signal $s_{tf}(nT)$ is passed through a linear channel it appears in the form

$$s_r(nT) = \mathrm{Re} \sum_k I_{tf}^k g((n-kL)T) \exp [j\omega_c nT + \theta(nT)] \quad (2)$$

Paper approved by the Editor for Communications and Modulation of the IEEE Communications Society. Manuscript received June 22, 1987; revised March 16, 1988. This work was supported by the Department of Defense. The views expressed are those of the authors and do not reflect the official policy or position of the U.S. Government.

The authors are with Lincoln Laboratory, Massachusetts Institute of Technology, Lexington, MA 02173-0073.

IEEE Log Number 8927624.

0090-6778/89/0600-0635$01.00

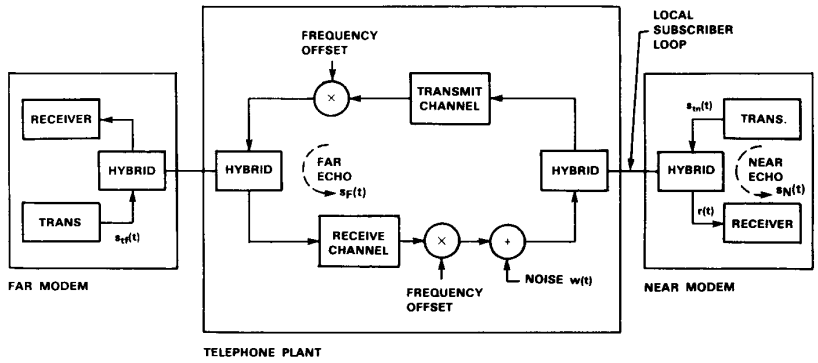

Fig. 1. Typical dialed telephone connection.

where $g(nT)$ is the composite baseband impulse response consisting of the convolution of the transmit pulse and the far-channel impulse response. The phase shift, $\theta(nT)$, added by the channel, is generally time-varying of the form

$$\theta(nT)=\omega_{ro}nT+\theta_{ro}(nT) \tag{3}$$

where the first term represents the phase change due to a frequency offset ω_{ro}, and the residual $\theta_{ro}(nT)$ may include a constant phase offset, phase hits, and phase jitter.

An expression similar to (2) can be written for the far echo with a corresponding symbol stream I_{tn}^{k} transmitted from the near end

$$s_F(nT)=\mathrm{Re}\sum_k I_{tn}^{k}g'[(n-kL)T]\exp[j\omega_c nT+\phi(nT)] \tag{4}$$

where the channel response and phase offset term of the far echo will be the result of passing through the channel in both directions. The phase is given by

$$\phi(nT)=\omega_{eo}nT+\phi_{eo}(nT) \tag{5}$$

where ω_{eo} is the frequency offset due to the far-echo channel. The near echo $s_N(nT)$ suffers only from the linear channel dispersion introduced by the local hybrid.

The total signal $r(nT)$ at the input to the demodulator of the near modem is the sum of four components

$$r(nT)=s_r(nT)+s_N(nT)+s_F(nT)+w(nT) \tag{6}$$

where the noise in the channel $w(nT)$ has a white component and may also include pulses of large amplitude, but small duration. The near echo can be as low as 9 dB below or as high as 40 dB above the far signal [3], [4], [9]. Although the far echo is typically 10 dB or more below the far signal, its level is still high enough that the far echo is the limiting factor in high rate (4800 bits/s and higher) transmission over standard dialed telephone lines [1]. Finally, the noise term is typically 20 or 30 dB below the far signal.

B. Traditional Modem Design

Fig. 2 shows how adaptive techniques [10]–[13] are applied to the traditional modem design which deals with the near echo and channel dispersion. The near-echo canceller is an adaptive transversal filter which generates an estimate $\hat{s}_N(nT)$ of the echo by operating on the transmitted symbols I_{tn}^{k}. The echo canceller is a transversal filter which produces a complex baseband representation of the echo which is then converted back to a passband signal for cancellation:

$$\hat{s}_N(nT)=\mathrm{Re}\,[\boldsymbol{x}^t(nT)\boldsymbol{a}(nT)\exp[j\omega_c nT]] \tag{7}$$

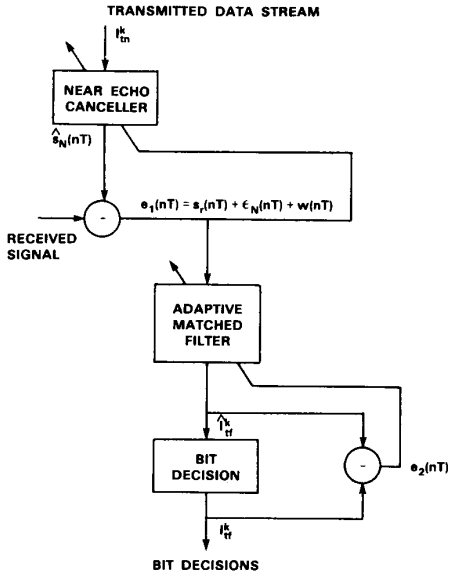

Fig. 2. Conventional modem design with near-echo canceller.

where $\boldsymbol{x}(nT)$ is a K dimensional vector made up of the complex data symbols residing in the echo canceller filter of length K at time nT, and $\boldsymbol{a}(nT)$ is the tap weight vector. For simplicity, the real operator and carrier modulation elements are not shown in Fig. 2 (this convention will be used henceforth).

The echo estimate, $\hat{s}_N(nT)$, is subtracted leaving an error

$$e_1(nT)=s_r(nT)+\epsilon_N(nT)+w(nT) \tag{8}$$

where the residual component of the near echo is given by

$$\epsilon_N(nT)=s_N(nT)-\hat{s}_N(nT). \tag{9}$$

The coefficients are updated using the well-known (LMS) gradient rule resulting from minimization of the power in $e_1(nT)$ [2], [10]

$$\boldsymbol{a}((n+1)T)=\boldsymbol{a}(nT)+\mu\boldsymbol{x}^*(nT)e_1(nT)\exp[-j\omega_c nT] \tag{10}$$

where μ is a constant which controls the rate of convergence. Since the inputs to the echo canceller are the symbol vectors I_{tn}^{k}, the filter will adapt to include in its impulse response the transmit weighting function $p(nT)$. The final impulse response will be the convolution of the echo channel with this window.

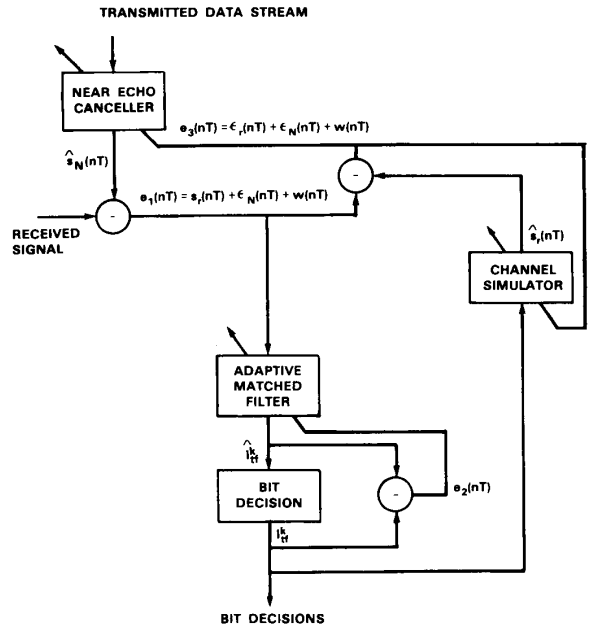

Fig. 3. Adaptive-reference echo canceller.

After demodulation by the carrier frequency, the error signal $e_1(nT)$ which contains the desired signal $s_r(nT)$ is also applied to the matched filter for the detection of the far signal. The output of the matched filter (consisting of complex coefficients) is a complex number $\hat{I}^k_{tf}$ which should approximate one of the points of the signal constellation of the transmitted signal. The bit decision I^k_{tf} is made by locating the nearest point in the signal constellation. By making the matched filter adaptive, we can also correct for the dispersion in the far signal. The adaptive matched filter thus acts as a far-channel equalizer [8]. The difference signal $e_2(nT)$ is computed between the actual filter output $\hat{I}^k_{tf}$ and the constellation point I^k_{tf}. This difference is used as the error signal to correct the matched filter characteristic with a gradient rule similar to (10), but with updates occuring at the baud rate [8].

With the system of Fig. 2, the near echo can be suppressed to a level below the far signal, but the adaptation is limited by the presence of the far signal component in the error signal to the echo canceller. By making the time constant long enough, we can begin to average out the effect of the far signal and further suppress the echo [6]. However, slowing the adaptation increases the acquisition time and makes the system slow in responding to changes in the channel characteristics.

III. Adaptive Reference Echo Cancellation

A. Canceller Structure

A more powerful way of dealing with the effect of the far signal on the cancellation process has been developed by Falconer [7] for near-echo cancellation. As shown in Fig. 3, Falconer introduces another transversal adaptive filter, the channel simulator, which creates an estimate $\hat{s}_r(nT)$ of the far signal $s_r(nT)$ based on the bit decisions made on the far signal. This estimate is subtracted from the error signal fed to the echo canceller. The residual error signal now contains, in place of $s_r(nT)$, only the error component

$$\epsilon_r(nT) = s_r(nT) - \hat{s}_r(nT) \tag{11}$$

so the total error $e_3(nT)$ reaching the control port of the echo canceller is

$$e_3(nT) = \epsilon_N(nT) + \epsilon_r(nT) + w(nT), \tag{12}$$

i.e., the sum of the near-echo and far-signal residuals and the noise source. In practice, a delay between the subtractor elements of Fig. 3 is required to account for the processing time through the matched filter and simulator. Without loss in generality, we assume this delay equals zero [7], [14], [15].

The generation of the far-signal estimate, also of the form of (7), is analogous to the creation of an echo estimate from the transmitted signal. The near-echo canceller and the channel simulator jointly try to minimize the power in the residual error $e_3(nT)$. This error minimization yields adaptive coefficient update procedures for each filter of the form of (10) where both adaptations are driven by the common error $e_3(nT)$ [7], [14], [15]. Both the near echo and far signal can be driven below the noise level so that the cancellation is limited only by the noise level and rate of adaptation.

B. The Problem of Frequency Offset

A problem with AREC arises when the channel introduces a frequency offset in the echo or in the desired far signal. A solution to this later problem, requiring a simple modification to the AREC structure in Fig. 3, motivates the new approach to cancelling far echos with frequency offset described in Section IV.

1) Far-Signal Frequency Offset: It is straightforward to correct far-signal frequency offset if the amount of offset is known. To obtain the far-end channel phase correction, we extend an approach [16], [17] which minimizes the power in $e_2(nT) = \hat{I}^k_{tf} - I^k_{tf}$ in Fig. 3 with respect to the unknown matched filter coefficients, denoted by the vector $\mathbf{c}(nT)$, and frequency offset ω_{ro}. We also allow for an unknown constant component to the phase compensation, $\theta(nT)$; i.e., $\theta(nT) = \omega_{ro}nT + \theta_{ro}$. We then jointly estimate this phase and the channel using a phase-locked loop (PLL), in addition to the equalizer [14], [16], [17].

$$\mathbf{c}((k+1)LT) = \mathbf{c}(kLT) + \beta e_2(kLT)\mathbf{z}(kLT) \tag{13}$$

$$\hat{\theta}((k+1)LT) = \hat{\theta}(kLT) + \hat{\omega}_{ro}(kLT) + k_1\Delta\xi(kLT) \tag{14}$$

with

$$\hat{\omega}_{ro}((k+1)LT) = \hat{\omega}_{ro}(kLT) + k_2\Delta\xi(kLT) \tag{15}$$

$$\Delta\xi(kLT) = \sin\left[\hat{\xi}(kLT) - \xi(kLT)\right] \tag{16}$$

where β controls the convergence of equalizer coefficients, where $\xi(kLT)$ and $\hat{\xi}(kLT)$ denote the phase of the complex far-end symbol I^k_{tf} and its estimate $\hat{I}^k_{tf}$, respectively, and the complex vector $\mathbf{z}(kLT)$, represents the input to the matched filter. Equations (14) through (16) represent a second-order phase-locked loop whose stability properties for a given k_1 and k_2 have been studied in [18], [19].

As illustrated in Fig. 4, this phase correction, $\hat{\theta}(nT)$, is used in three ways. First, it is used to eliminate the carrier frequency of the signal into the matched filter. Second, it is used to shift the output of the channel simulator in the opposite direction so that the carrier frequency of the signal from the channel simulator is shifted to match the carrier frequency of the received signal. Finally, it is used to correct the error signal controlling the adaptation of the simulator. These later two phase modifications result from minimization of the residual error $e_3(nT)$ when the frequency and phase offsets are specified [14].

2) Far-Echo Frequency Offset: With frequency offset present in the far echo, the canceller tap weights of Fig. 3 rotate in an attempt to track the linearly advancing phase. The canceller's complex taps will track the channel impulse

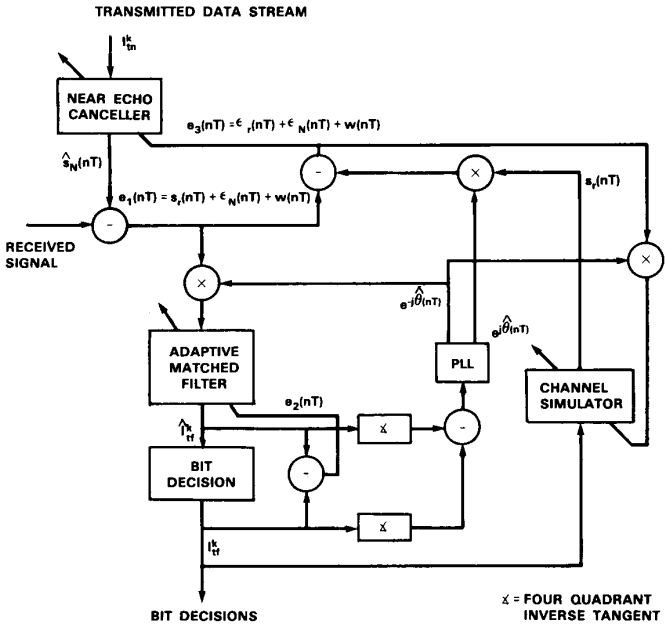

Fig. 4. Adaptive-reference canceller with corrections for frequency offset in far-end signal.

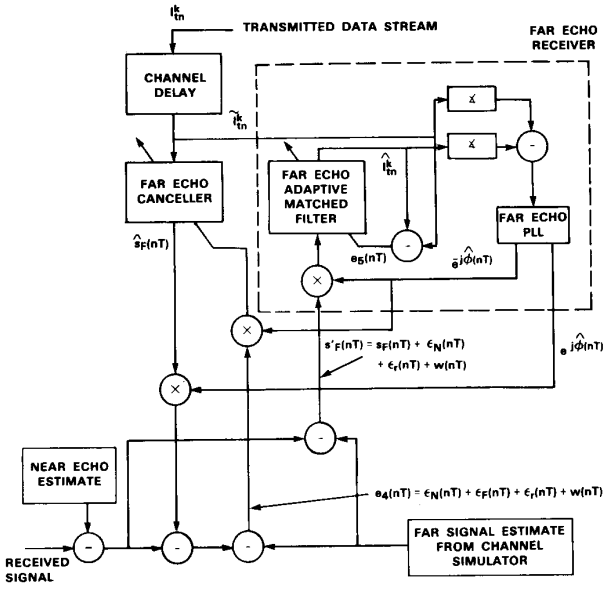

Fig. 5. Far-echo cancellation and frequency offset estimation.

response with a fixed-phase lag which prevents the cancellation from reaching adequate suppression (see simulations in Section V-B).

Estimating the frequency offset of the far echo is difficult because the far echo is masked by the stronger far signal and near echo. The following Section IV shows that by enhancing the far echo in the presence of these interferences, the approach to far-signal frequency offset estimation, given above, can be extended to the far-echo frequency offset.

IV. Cancellation with Far-Echo Frequency Offset

A. Canceller Structure

A separate canceller for the far echo is illustrated in Fig. 5. This canceller operates on a delayed version of the transmitted symbols $\tilde{I}^k_{in}$ to produce a replica $\hat{s}_F(nT)$ of the far echo with the form of (7). Since the far echo is masked by the stronger far signal and near echo, to estimate the frequency offset of the far echo, we must first enhance its visibility relative to these

signals. Fig. 5 shows how this can be done. The complete received signal, in sampled data form, is as in (1)

$$r(nT) = s_r(nT) + s_N(nT) + s_F(nT) + w(nT). \quad (17)$$

We have already generated an estimate $\hat{s}_r(nT)$ of the far signal $s_r(nT)$ and an estimate $\hat{s}_N(nT)$ of the near echo $s_N(nT)$ via the structure in Fig. 3. By subtracting these estimates, we obtain a far echo estimate $s_F'(nT)$ which consists of the far echo, the noise, and two residuals

$$s_F'(nT) = s_F(nT) + \epsilon_N(nT) + \epsilon_r(nT) + w(nT). \quad (18)$$

In practice, the received signal, with $\hat{s}_N(nT)$ removed, must be delayed prior to determining the far-echo estimate $s_F'(nT)$ to account for the processing time required by the channel equalizer and channel simulator.

The error residual $e_4(nT)$ driving the adaptation of the far-echo canceller coefficients consists of the noise and three residuals due to far-signal, far-echo, and near-echo estimates

$$e_4(nT) = \epsilon_N(nT) + \epsilon_F(nT) + \epsilon_r(nT) + w(nT) \quad (19)$$

where the far-echo residual $\epsilon_F(nT)$ is given by

$$\epsilon_F(nT) = s_F(nT) - \hat{s}_F(nT). \quad (20)$$

As described further in the following Section IV-B, the error residual $e_4(nT)$ is also used to drive the adaptation of the near-echo and channel-simulator coefficients.

To estimate the frequency offset ω_{eo} and resulting phase correction $\phi(nT)$ of (5), $s_F'(nT)$ is fed to a receiver structure similar to that used for demodulating the far signal in (13)–(16). The signal $s_F'(nT)$ is first fed to the far-echo adaptive-matched filter which attempts to demodulate the echo signal. Although the level of the far echo may not be high enough above the noise to permit reliable demodulation, this is not important. On the far-signal receiver channel we used complex vectors from the matched filter output to make bit decisions, but this is not necessary here. Since we are processing an echo, the bit pattern which produced the echo is already known at the receiver. This known bit pattern is used to compute the error signal which is used to control the adaptation of the matched filter and provide the input to the PLL which determines the frequency offset. The adaptation of this matched filter corrects for the dispersion in the far echo. Since the far echo has traversed a different channel than the far signal, this correction is made independently of the correction in the far-signal receiver.

To obtain the far-end-channel phase correction, we minimize the power in $e_5(nT) = \hat{I}_{tn}^k - \tilde{I}_{tn}^k$ with respect to the unknown matched filter coefficients, denoted by the vector $\boldsymbol{d}(nT)$, and frequency offset ω_{eo}. We also allow for an unknown constant component to the phase compensation, $\phi(nT)$, i.e., $\phi(nT) = \omega_{eo}nT + \phi_{eo}$. The joint adaptive matched filter and PLL is then given by [14], [16], [17].

$$\boldsymbol{d}((k+1)LT) = \boldsymbol{d}(kLT) + \beta e_5(kLT)\boldsymbol{v}(kLT) \quad (21)$$

$$\hat{\phi}((k+1)LT) = \hat{\phi}(kLT) + \hat{\omega}_{eo}(kLT) + k_1 \Delta\xi(kLT) \quad (22)$$

with

$$\hat{\omega}_{eo}((k+1)LT) = \hat{\omega}_{eo}(kLT) + k_2 \Delta\xi(kLT) \quad (23)$$

$$\Delta\xi(kLT) = \sin\,[\hat{\xi}(kLT) - \xi(kLT)] \quad (24)$$

where $\xi(kLT)$ and $\hat{\xi}(kLT)$ denote the phase of the delayed complex near-end symbol $\tilde{I}_{tn}^k$ and its estimate $\hat{I}_{tn}^k$, respectively, and the complex vector, $\boldsymbol{v}(kLT)$, represents the phase-corrected input to the matched filter. The stability of (21)–(24) is guaranteed with the approximate choice of k_1, k_2, and β.

The phase correction for the far-echo canceller is applied in the same way as in the channel simulator. It is removed from the signal going to the far-echo matched filter, added back into the signal coming out of the far-echo canceller so that its carrier frequency will match that of the far-echo component in the received signal, and also applied to the error signal controlling the adaptation of the far-echo canceller. These later two phase modifications result from minimization of the residual error $e_4(nT)$ when the frequency and phase offsets are specified [14].

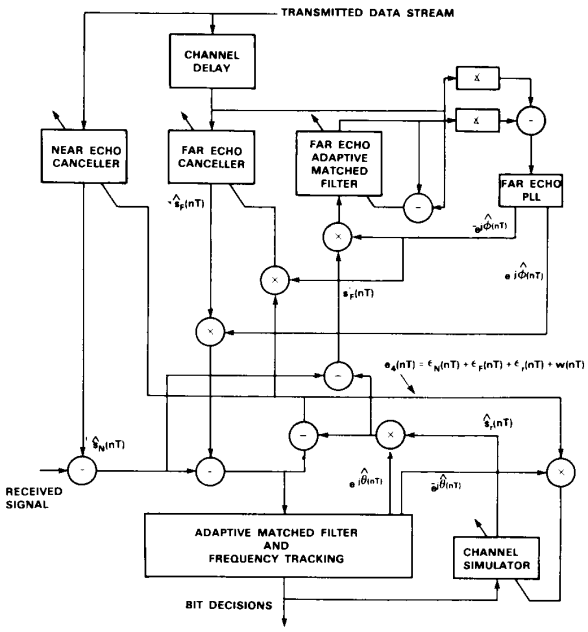

Fig. 6. Canceller with correction for far-echo and far-signal frequency offset.

B. The Composite System

The system integrating the modem design of Fig. 4 with the new far-echo canceller and associated receiver structure of Fig. 5 is illustrated in Fig. 6. The far-signal receiver which generates the far-signal phase correction $\hat{\theta}(nT)$ and the far-echo receiver which generates the far-echo phase correction $\hat{\phi}(nT)$ are given by (14) and (22), respectively. The coefficients of the near-echo canceller, $\boldsymbol{a}(nT)$, the far-echo canceller, $\tilde{\boldsymbol{a}}(nT)$, and the channel simulator, $\boldsymbol{b}(nT)$, are jointly adapted and driven by the common error residual $e_4(nT)$

$$\boldsymbol{a}((n+1)T) = \boldsymbol{a}(nT) + \mu \boldsymbol{x}^*(nT) e_4(nT) \exp\,[-j\omega_c nT] \quad (25)$$

$$\tilde{\boldsymbol{a}}((n+1)T) = \tilde{\boldsymbol{a}}(nT) + \mu \tilde{\boldsymbol{x}}^*(nT) e_4(nT) \cdot \exp\,[-j(\omega_c nT + \hat{\phi}(nT))] \quad (26)$$

and

$$\boldsymbol{b}((n+1)T) = \boldsymbol{b}(nT) + \mu \boldsymbol{y}^*(nT) e_4(nT) \cdot \exp\,[-j(\omega_c nT + \hat{\theta}(nT))] \quad (27)$$

where the residual $e_4(nT)$ is mixed by three distinct factors before driving the various coefficient adaptations where $\boldsymbol{x}(nT)$, $\tilde{\boldsymbol{x}}(nT)$, and $\boldsymbol{y}(nT)$ represent the data vectors residing in each filter, respectively, and where for simplicity we have

assumed the same feedback gain μ for all three adaptations. These three joint adaptations can be derived by minimization of the power in the residual $e_4(nT)$ when the phase corrections are specified [14].

C. Performance Analysis

The steady-state performance of this composite canceller has been analyzed [14] using a method which extends the analysis done by Falconer [7] for the adaptive reference near-echo canceller with bipolar symbols. Since the phase corrections $\phi(nT)$ and $\theta(nT)$ are time-varying and depend on their respective receiver structures, the dynamic performance is difficult to analyze and beyond the scope of this study.

Assuming that the frequency and phase offset estimates comprising the phase corrections have settled, it has been shown that the joint adaptation given by (25)–(27) is stable [14]. In particular, with unity power in the transmit and receive symbols, it can be shown that the steady-state signal-to-echo ratio at the input to the matched filter for the far-signal receive data channel is given approximately by

$$\frac{S}{E}=\frac{P_r}{P_w}\frac{[2-\mu(2N_a+N_b)]}{2\mu N_a} \tag{28}$$

where P_r is the power in the received far-end signal $s_r(nT)$, P_w is the power in the additive channel noise, N_a is the length of the adaptive filter for the cancellers, N_b is the length of the filter in the channel simulator, and μ is the convergence parameter in (25)–(27). The final level of the echo relative to the signal is independent of the original level of the echo. This means that the final level for the echo is only a function of the signal-to-noise ratio and the convergence parameter μ. The suppression of the echo can be made arbitrarily large by reducing μ. This corresponds to increasing the averaging time of the filters. The parameter μ must also be small enough to keep the numerator of the expression positive if the filters are to remain stable.

V. Evaluation

A. Simulation

A simulation of the algorithm of Fig. 6 was performed to verify the steady-state performance predictions, assess the stability of the algorithm, and to test the performance on other types of interference which are not easily modeled analytically. The simulation was written for a VAX11/780 computer using floating-point arithmetic. The simulated data rate was 4800 bits/s using four-phase differential phase shift keying (DPSK) [8]. The detailed parameters of the modem and simulation are given in Table I. A telephone channel with average dispersion (about 7 ms) was used for both directions of the channel, as well as for the near-echo path, representing a worst case scenario for the later path. The adaptive filters in the echo cancellers and channel simulator are sufficiently long to represent the composite signal formed by convolving the transmit pulse with their respective channels.

The receiver's adaptive structures are started sequentially during a 2000 baud training preamble. In the simulation, it was assumed that the time delay of the far-echo delay was known. The preamble adaptation process was run with both modems running simultaneously. The timing scenario for adaptation over this preamble was determined according to the relative levels and is illustrated in Fig. 7. Since the near echo is the largest contribution to the received signal, the near-echo canceller adaptation begins at the onset of operation. After 700 bauds, following reduction of the near echo, the far-end-channel equalizer and its associated phase-locked loop (PLL) are started. AT 1000 bauds the channel-simulator adaptation is begun. This gives the phase-locked loop some time to estimate a frequency offset to be used by the channel simulator which

TABLE I
DESIGN SPECIFICATIONS FOR NEAR/FAR-ECHO-CANCELLING MODEM ALGORITHM

Modem Signal Specifications	
Signal Constellation:	Four-Phase DPSK [8]
Baud Rate:	2400 Bd/s
Sampling Rate:	7200 Hz
Carrier Frequency:	1800 Hz
Transmit Pulse:	31 Point (raised cosine spectrum[8]
Bit Rate:	4800 b/s
Preamble:	2000 Bd
Receiver Specifications	
Adaptive Filter Lengths	N = 88 taps
Near Echo/Far Echo Canceller and Simulator Convergence Gains:	μ = .004
Far-Signal and Far-Echo Matched Filter Convergence Gains:	β = .15
Phase-Lock Loop Parameters	k_1 = 1/64, k_2 = 1/16384 (critically damped)

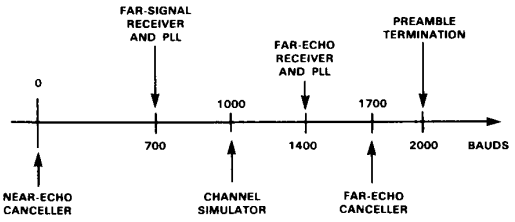

Fig. 7. Preamble timing scenario for near/far-echo-cancelling modem algorithm.

starts its adaptation at 1000 bauds, and also allows time to make the far echo visible over the near echo and far-end signal. The far-echo equalizer and its associated PLL are started at 1400 bauds, followed finally by the far-echo canceller at 1700 bauds. The far echo is cancelled last, since it is the smallest of the received signal components.

B. Frequency Offset in the Far-Echo Channel

In order to compare the new algorithm to the adaptive-reference algorithm of Section IV, we first test the system with no near echo and with no frequency offset in the far-end signal. The near-echo canceller and the far-end channel phase correction $\phi(nT)$ in the simulation were both disabled. A 2 Hz frequency offset was injected into the far echo at 3000 bauds, the echo-to-far-end-signal ratio is -10 dB and the far-end signal-to-noise ratio is 20 dB. Fig. 8 shows that the introduction of a 2 Hz frequency offset at 3000 bauds caused a marked initial decrease in suppression which results in a transient increase in decision errors. Nevertheless, the phase-locked loop quickly tracked the frequency offset and recovered the original suppression within about 0.5 s.

Fig. 9 shows the far signal-to-echo ratio at the input to the matched filter when using the conventional adaptive reference canceller (Fig. 3) with the above 2 Hz echo frequency offset.

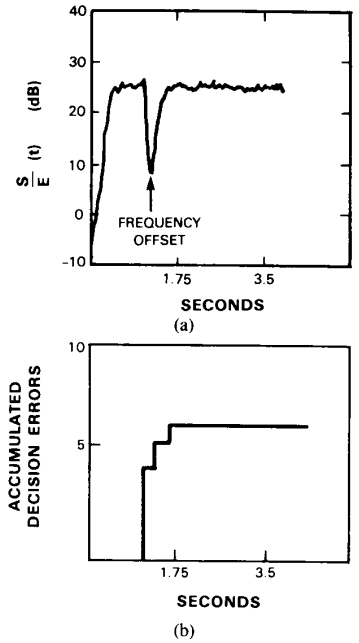

Fig. 8. Performance of adaptive reference far-echo cancelling modem algorithm (no near echo). (a) Signal-to-echo ratio at far-signal matched filter input. (b) Decision errors by far-signal receiver.

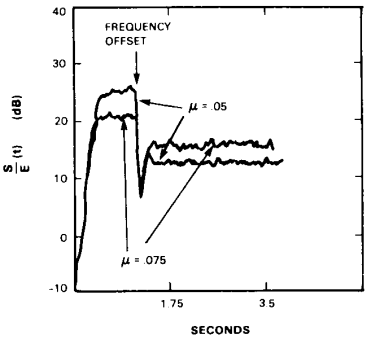

Fig. 9. Effect of convergence gain on conventional AREC with far-echo frequency offset.

The canceller's complex taps track the channel impulse response with a fixed-phase lag which prevents the cancellation from reaching the high suppression level prior to injection of frequency offset. As shown in Fig. 9, an increase in the convergence gain to $\mu = 0.075$ tends to increase the echo suppression during the frequency offset by improving the tracking capability of the canceller; however, the echo suppression is worse before the introduction of the frequency offset. The new echo-suppression method has improved echo suppression by almost 13 dB over the conventional AREC.

C. The Composite System

An extensive set of simulations was run to test the performance of the composite system against both white Gaussian noise and other channel distortions such as phase discontinuities and impulse noise. The complete results are described elsewhere [14]. We present here some representative cases. Fig. 10 shows the result from the case with frequency offset of 2 Hz (set for all time) in only the far echo with a near echo-to-signal ratio of 30 dB, a far echo-to-signal ratio of -10 dB, and $S/N = 30$ dB and 20 dB. All five adaptive filters successfully converged—two adaptive cancellers, the channel simulator, and the two adaptive equalizers, along with joint convergence of the phase-locked loop for estimation of the far-echo frequency offset. Fig. 10 shows the dynamic performance of the canceller for this case. The most important consideration is, of course, the ability of the system to demodulate the incoming data. Fig. 10(a) shows the signal-to-echo ratios at the input to the far-channel equalizer/matched filter. The suppression of the near echo starts immediately and continues until it is a few decibels below the noise. The suppression of the far echo is delayed until the near echo has

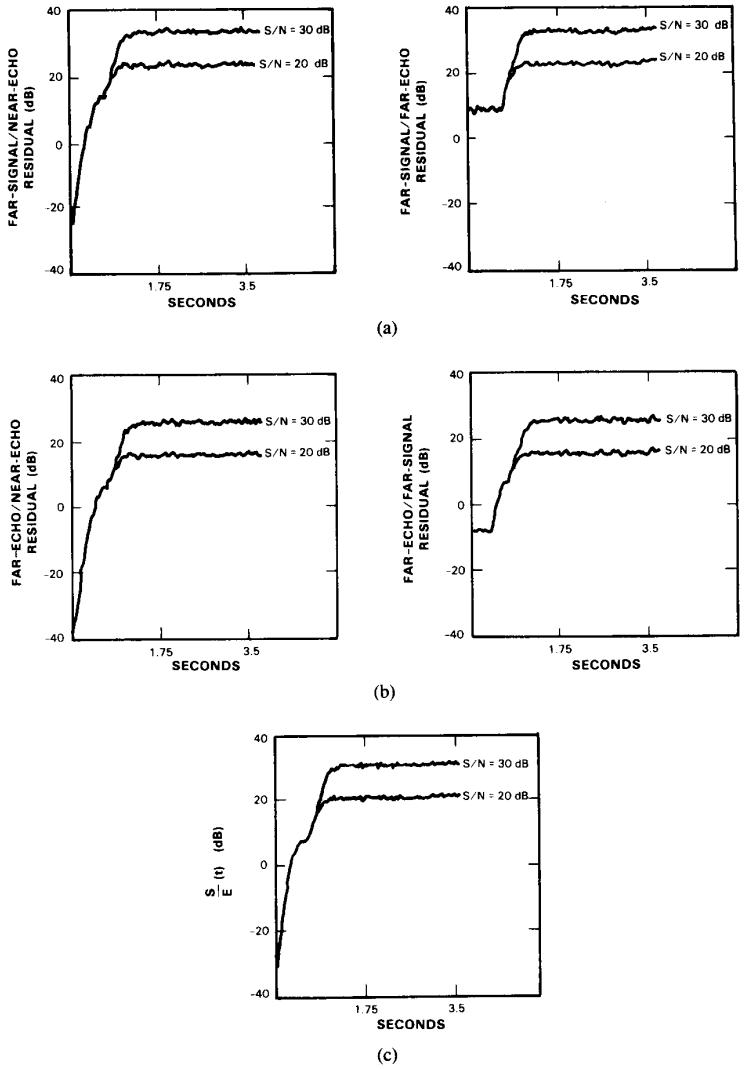

Fig. 10. Error residuals of modem algorithm with frequency offset in far-echo path. (a) Residuals with respect to far signal at far-signal receiver. (b) Residuals with respect to far echo at far-echo receiver. (c) Signal-to-echo residual at equalizer input.

been suppressed. It is then quickly suppressed to about the same level. Fig. 10(b) shows the suppression achieved at the input to the far-echo receiver; the interfering signals are the near-echo and far-end signal. Again, the amount of suppression achieved depends on the noise level. Fig. 10(c) shows the combined near- and far-echo residual relative to the far-end signal at the far-channel equalizer input; i.e., S/E, the signal-to-echo residual ratio which governs the utlimate error rate of the modem design. The steady-state results of Fig. 10(c) approximately match those predicted from expression (28); for $S/N = 30$ dB we obtain a measured $S/E \approx 30.6$ dB, close to the predicted 31.1 dB, and for $S/N = 20$ dB we obtain a measured $S/E \approx 20.7$ dB, also close to the predicted 21.1 dB.

Fig. 11 shows the case with a frequency offset of 2 Hz in both the far signal and the far echo. Fig. 11(a) and (b) give the estimated frequency offsets in both signals as a function of time during the convergence of the preamble, while Fig. 11(c) shows the signal-to-echo ratio at the input to the receiver matched filter. In these experiments the near-echo-to-signal ratio was 20 dB and the far-echo-to-signal ratio was -10 dB. Convergence within the preamble time was obtained with values of S/N down to about 10 dB and near-echo-to-signal ratios up to 60 dB.

The system was also tested against sudden discontinuities in the channel phase such as might result from cycle slippage in the carrier telephone plant and against impulse noise [14]. In both cases, the system recovers quickly in spite of decision errors by the far-signal receiver and reacquires the signal correctly. One example is given in Fig. 12 where unidirectional phase hits introduced in the far echo are 30, 80, and 180°, beginning at 3.7 s, and occuring in that order with about a 4 s spacing. The far-echo phase hits are denoted in Fig. 12 by ϕ_k. The phase hits in the far-end signal are 15, -40, and 135°, beginning at about 1.6 s, and occurring in that order with about a 4 s spacing. The far-signal phase hits are denoted in Fig. 12 by θ_k. Impulse noise with about twice the amplitude of the far-end signal and with a width of one baud was also introduced at a rate of 5 pulses/s. All other conditions were as in the previous example with $S/N = 20$ dB. The decision error rate in Fig. 12(b) is roughly 10/s, which is the number

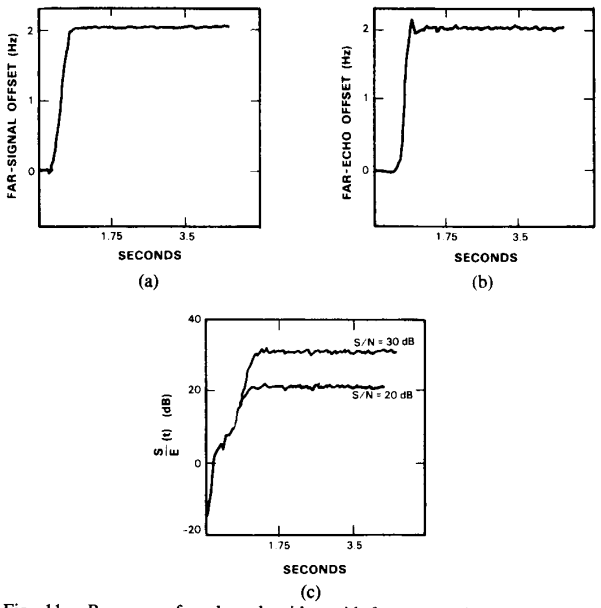

Fig. 11. Response of modem algorithm with frequency offset in far-signal and far-echo paths. (a) Far-signal frequency offset estimate with $S/N = 30$ dB. (b) Far-echo frequency offset estimate with $S/N = 30$ dB. (c) Signal-to-echo residual at far-signal equalizer input.

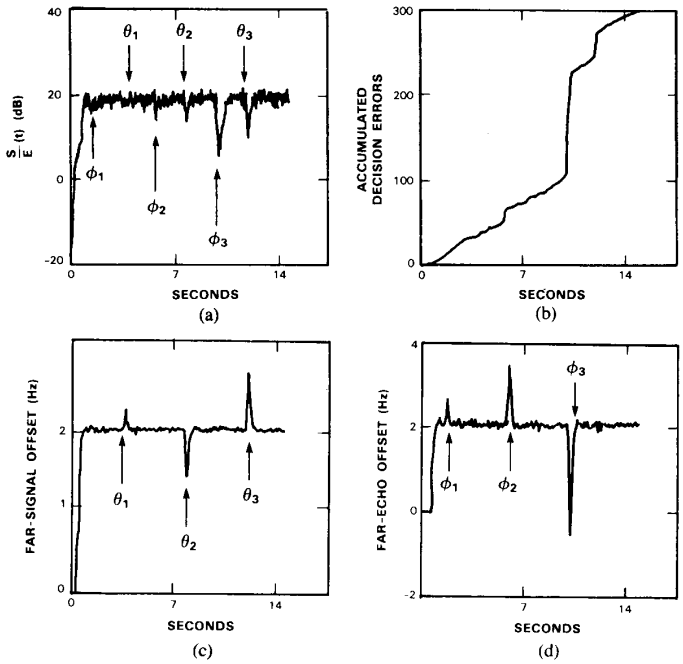

Fig. 12. Performance of complete modem with phase hits and impulse noise. (a) S/E, (b) accumulated receiver errors, (c) far-end signal frequency offset estimate, (d) far-echo frequency offset estimate.

expected with the 5/s impulse rate, assuming each impulse affects two DPSK symbols.

VI. Conclusions

We have described a full-duplex LMS adaptive reference echo-cancelling modem which accounts for both near and far echo. The adaptive reference technique generates an estimate of the far-end signal which is used to obtain improved estimates of the near and far echoes. Estimation of the frequency offset in the far echo uses a separate receiver structure devoted to demodulation of the far echo and tracking its frequency offset. The structure can equally as well handle

frequency offset in the far signal. When simulated at 4800 bits/s this algorithm was experimentally demonstrated to be robust and stable for both Gaussian and impulse noise and for phase hits in the channel. The steady-state behavior of the simulated system closely matched that predicted analytically. Analysis of the dynamic performance of the adaptive system awaits further study.

Additional future research may also include developing a passband version of the (currently baseband) echo-cancelling modem design. This system will have additional importance at 9600 bits/s where other distortions may require attention as, for example, phase jitter. It appears that estimating and compensating for such distortions should not pose a problem. Finally, simulations with channel bit errors should be performed to prove the ultimate feasibility of the new modem design.

Acknowledgment

The authors would like to thank J. Proakis, D. Messerschmitt, R. Cohn, D. Rahikka, and R. Dean for helpful discussions.

References

[1] J. J. Werner, "Effects of channel impairments on the performance of an in-band data-driven echo canceller," *AT&T Tech. J.*, vol. 64, no. 1, Jan. 1985.
[2] S. B. Weinstein, "A passband data-driven echo canceller for full-duplex transmission on two-wire circuits," *IEEE Trans. Commun.*, vol. COM-25, July 1977.
[3] M. B. Carey *et al.*, "1982/83 end office connection study: Analog voice and voiceband data transmission performance characterization of the public switched network," *Bell Syst. Tech. J.*, vol. 63, pp. 2059–2119, Nov. 1984.
[4] L. M. Manhire, "Physical and transmission characteristics of customer loop plant," *Bell Syst. Tech. J.*, vol. 57, pp. 35–59, Jan. 1978.
[5] P. H. Wittke, S. R. Penstone, and R. S. Keightley, "Measurements of echo parameters pertinent to high-speed full-duplex data transmission on telephone circuits," *IEEE J. on Select. Areas Commun.*, vol. SAC-2, Sept. 1984.
[6] R. D. Gitlin and S. B. Weinstein, "The effects of large interference on the tracking capability of digitally implemented echo cancellers," *IEEE Trans. Commun.*, vol. COM-26, June 1978.
[7] D. D. Falconer, "Adaptive reference echo cancellation," *IEEE Trans. Commun.*, vol. COM-30, Sept. 1982.
[8] J. G. Proakis, *Digital Communications*. New York: McGraw-Hill.
[9] D. Messerschmitt, "Tutorial on hybrid method full duplex data transmission," Lincoln Lab., Int. Memo, Apr. 1984.
[10] B. Widrow and S. D. Stearns, *Adaptive Signal Processing*. Englewood Cliffs, NJ: Prentice-Hall.
[11] K. H. Mueller, "A new digital canceller for two-wire full-duplex data transmission," *IEEE Trans. Commun.*, vol. COM-24, Sept. 1976.
[12] J. Werner, "An echo-cancellation based 4800 bps full-duplex DDD modem," *IEEE J. Select. Areas Commun.*, vol. SAC-2, Sept. 1984.
[13] M. M. Sondhi and D. A. Berkley, "Silencing echoes on the telephone network," *Proc. IEEE*, vol. 68, Aug. 1980.
[14] T. F. Quatieri and G. C. O'Leary, "Adaptive-reference near- and far-echo cancellation in the presence of frequency offset," *Tech. Rep.* 771, Lincoln Lab., M.I.T., May 1987.
[15] ——, "Decision-directed echo cancellation for full-duplex data transmission at 4800 bps," IEEE 1986 Int. Conf. Acoust., Speech, Signal Processing, Tokyo, Japan, Apr. 1986.
[16] D. D. Falconer, "Jointly adaptive equalization and carrier recovery in two-dimensional digital communication systems," *Bell Syst. Tech. J.*, vol. 55, no. 3, Mar. 1976.
[17] ——, "Analysis of a gradient algorithm for simultaneous passband equalization and carrier phase recovery," *Bell Syst. Tech. J.*, vol. 55, no. 4, Apr. 1976.
[18] R. D. Gitlin and J. S. Thompson, "A phase adaptive structure for echo cancellation," *IEEE Trans. Commun.*, vol. COM-26, Aug. 1978.
[19] A. J. Viterbi, *Principles of Coherent Communications*. New York: McGraw-Hill, 1966.

★

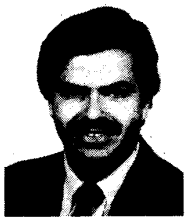

Thomas F. Quatieri (S'73–M'79–SM'87) was born in Somerville, MA, on January 31, 1952. He received the B.S. degree (summa cum laude) from Tufts University, Medford, MA, in 1973, and the S.M., E.E., and Sc.D. degrees from the Massachusetts Institute of Technology (M.I.T.), Cambridge, 1975, 1977, and 1979, respectively.

In 1980, he joined the Sensor Processing Technology Group of M.I.T., Lincoln Laboratory, Lexington, MA, where he worked on problems in multidimensional digital signal processing and image processing. Since 1983 he has been a member of the Speech Systems Technology Group at Lincoln Laboratory where he has been involved in digital signal processing for speech enhancement, speech coding, and data communications. He has contributed many publications to journals and conference proceedings, written several patents, and co-authored chapters in two edited books: *Advanced Topics in Signal Processing* (Prentice-Hall, 1987) and *Programs for Digital Signal Processing* (IEEE Press, 1979).

Dr. Quatieri is the recipient of the 1982 Paper Award of the IEEE Acoustics, Speech, and Signal Processing Society for the paper, "Implementation of 2-D Digital Filters by Iterative Methods." This award is given for the best paper by an author under thirty years of age. He is a member of the IEEE Digital Signal Processing Technical Committee, and since 1983 has served on the steering committee for the bi-annual Digital Signal Processing Workshop. He is also a member of Tau Beta Pi, Eta Kappa Nu and Sigma Xi.

★

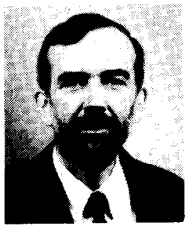

Gerald C. O'Leary (M'66) received the B.S., M.S., and Electrical Eng. degrees from the Electrical Engineering Department of the Massachusetts Institute of Technology in 1963, 1964, and 1966.

Since then, he has worked for the MITRE Corporation, Bedford, MA; Signal Processing Systems, Inc., Waltham, MA; and in 1977 he joined the M.I.T. Lincoln Laboratory, Lexington, MA. Since 1984 he has been Assistant Group Leader of the Speech Systems Technology Group at Lincoln Laboratory. His professional interests include signal processing, speech, and real-time architectures for digital signal processing.